Burnout Correlations for Even - and Odd-Numbered Peripheral Rod Clusters over Low Pressure Range

E. H. K. Akaho, *BSc, MSc, PhD, Dic*
Department of Nuclear Engineering
National Muclear Research Institute
Ghana Atomic Energy Commission
Accra-Ghana

ABSTRACT

Burnout data with low pressure Freon-113 for even- and odd- numbered peripheral rod clusters with relatively large spacings were used to derive equations in terms of dimensionless parameters suggested by Barnett. The equations which are for three different flow regimes for each rod geometry (even or odd) were found to predict burnout data with maximum RMS deviation being 3.8%.

INTRODUCTION

For large rod spacings, burnout data and correlations are practically nonexistent. Based on experiments in a simpler annular geometry, Bernath [1] derived a set equations which sometimes applied to rod bundles with large spacings but it is still not clear if these equations are applicable for the latter case.

In a preceding study Berger and Akaho [2] reported burnout results for Freon-113 obtained in a low pressure range of 101.3 - 165kPa (ρ_l/ρ_v = 205 - 113) for even- and odd-numbered peripheral rod clusters as illustrated in Figure 1. The rods with a diameter of 4.76mm were uniformly spaced in the free flow area. The geometrical characteristics of the tested clusters are listed in Table 1. The spacings are relatively large, 3.14 - 11.03mm. Significant differences in the behaviour of burnout conditions were noticed for evens and odds. These observations are found to be consistent with those made by Macbeth [3]. For each geometry, three flow regimes called A-(burnout of dryout type), C-(burnout in nucleate boiling) and B-(intermediate between A and C) were identified, which is consistent with earlier investigations of Katto [4] and Dukler [5].

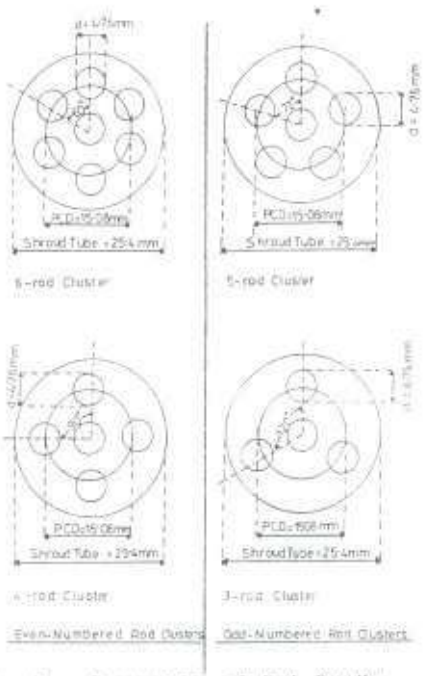

Fig 1: Cross-section of Rod Bundles with Unheated Central Rods.

Apart from the C-region for even-numbered clusters the burnout data followed the single linear ϕ_h-ΔH_i relationship as discussed for instance in Collier's book [6]. In the C-region for evens there occurred a change of slope of the ϕ_h-ΔH_i lines as also noticed by Kirby et al [7] with low pressure water in annular geometry.

The exit quality, χ_{ex} for a given ΔH_i and mass flow rate m was determined from the energy balance on the test section as:

$$\chi_{ex}=\left[\frac{Q_b}{\dot{m}H_{fg}}\right]-\left[\frac{\Delta H_i}{H_{fg}}\right] \qquad (1)$$

Dr. E. H. K. Akaho

Table 1: **Characteristics of Tested Clusters.**

	Units	Rod Cluster			
		6	5	4	3
PCD x 10^3	m	15.08	15.08	15.08	15.08
A_f x 10^6	m	382.14	399.78	418.00	435.58
P_h x 10^3	m	89.72	74.78	59.82	44.86
A_h x 10^6	m	44.86	37.39	29.91	22.42
a_r	%	29.15	22.96	18.19	13.84
d_h x 10^3	m	17.04	21.38	27.95	38.84
d_e x 10^3	m	14.61	17.82	22.36	29.13
l_h/d_h	-	29.35	23.38	17.89	12.87
p/d	-	1.66	1.99	2.49	3.32

The variation of burnout in the low pressure range was found to follow an exponential relationship of the simple form:

$$\frac{\phi_b}{\phi_{b1}} = \left[\frac{P}{P_1}\right]^{\alpha} \quad (2)$$

where α is different for the various flow regimes but of equal value if the geometry of rod cluster (even or rod) is the same.

In this report the burnout data are correlated in terms of dimensionless parameters that can be found in the scaling laws derived by Barnett [8]. The method of analysis with the simplifying assumptions which made the derivation of equations possible is explained. The boundaries between the flow regimes are established. Also, discussed is the criterion for determining the exit quality at which a break will occur in the burnout-exit quality relationship in the C-regime. The equations derived from experiments with Freon -113 burnout data were used to predict water data and the possibility of applying them to other saturated liquids was considered.

2. CORRELATING EQUATIONS

Barnett [8] suggested the following relationship for burnout in saturated flows:

$$\frac{\phi_b \gamma^{1/2}}{H_{fg}\rho_l^{1/2}} = f\left(\frac{G\gamma^{1/2}}{\rho_l^{1/2}}, \frac{\rho_l}{\rho_v}, \frac{\Delta H_i}{H_{fg}}, \frac{l_h}{d_h}, \frac{\phi_b c_{pl} \rho_l^{1/2}}{k_l \gamma^{1/2}}\right) \quad (3)$$

The dimensionless parameters should permit the modelling of burnout results from one saturated fluid to another, e.g. from Freon-113 to water. They were later found to be suitable also for scaling burnout fluxes in subcooled Freon-113 [9]. To adapt the expression for the present case the following assumptions were made:

(a) The last dimensionless group was neglected since, in the tested range of pressure, the variations of cp_l and k_l were small and the other terms appear in the remaining groups. This is also consistent with the findings of Jones and Hoffman [10] and of Aladevev et al [11] that cp_l and k_l are unimportant and have no effect on ϕ_b.

(b) It was earlier stated that the ϕ_b values follow a linear relationship with ΔH_i. Therefore we can write

$$\phi_b = \phi_b^o + K\frac{\Delta H_i}{H_{fg}} \quad (4)$$

which can be expressed in the form

$$\phi_b = \phi_b^o\left(1 + K\frac{\Delta H_i}{H_{fg}}\right) \quad (5)$$

where $K = \kappa/\phi_b^o$ and ϕ_b^o is the burnout flux at zero subcooling ($\Delta H_i = 0$) which can be correlated in the form:

$$\frac{\phi_b^o \gamma^{1/2}}{H_{fg}\rho_l^{1/2}} = f\left(\frac{G\gamma^{1/2} p}{\rho_l^{1/2} p_1}, \frac{\rho_l}{\rho_v}, \frac{l_h}{d_h}\right) \quad (6)$$

The term $G\gamma^{n}/\rho_l^{n}$ from Eqn. (3) was modified to $G\gamma^{n}p/\rho_l^{n}p_1$ because it was found that $G\gamma^{n}p/\rho_l^{n}p_1$ remains fairly constant for a particular coolant within the test pressure range i.e for Freon-113 in the range of 101.3 - 165kPa. This applies to other coolants i.e. H_2O, Freon-112, NH_3 and Hg for

density ratio in the range ρ_l/ρ_v = 205 - 125. Thus, it becomes possible to vary the parameter $G_v^n p/\rho_l^n p_l$ while ρ_l/ρ_v (pressure dependent) and l_b/d_h were kept constant.

(c) The number of l_b/d_h ratio in the tested clusters was limited to two for each of the rod configurations (even or odd). Therefore, it had to be assumed that the dependence on l_b/d_h was hyperbolic as found by earlier researchers [4, 12].

Consequently,

$$\phi_b^n = f\left[\frac{1}{a+b(l_b/d_h)}\right] \qquad (7)$$

The ϕ_b^* term appearing on the RHS of Eqn. (5) can be correlated in terms of the parameters suggested in Eqn. (6) which is finally expressed as:

$$\frac{\phi_b^n \gamma^{1/2}}{H_{fg}\rho_l^{1/2}} = \frac{f\left[\frac{G_v^{1/2}p}{\rho_l^{1/2}p_l}\right] \times f\left[\frac{l_b}{d_h}\right]}{f\left[\frac{\rho_l}{\rho_v}\right]} \qquad (8)$$

The ϕ_b^* data were obtained from the intersects of the $\phi_b \Delta H_i$ lines with the ϕ_b - axis. In view of the difficulties in maintaining $\Delta H_i = 0$, the extrapolated values were used instead of direct measurements. The ϕ_b^* data expressed in the dimensionless form as on the LHS of Eqn. (6) was plotted against $G_v^n p/\rho_l^n p_l$ for fixed ρ_l/ρ_v (and hence fixed pressure) and for a given cluster yielded a curve with different slopes in the flow regimes. The graphical representation of the ϕ_b^* data for the 6-rod (even) and 5-rod are presented in Figs. 2 and 3 respectively. It was for each cluster geometry according to Eqn. (6).

The form of Eqn.(5) is valid in all flow regimes except for the even-clusters in the C-regime which is characterised by high flow rates. Here, the dependence of ϕ_b on $(\Delta H_i/H_{fg})$ is represented by straight lines with different slopes called K_L and K_H. The subscripts L and H denote low and high enthalpies respectively. In the H-regime a factor β was required to account for the change of slope of the ϕ_b - ΔH_i line. Eqn. (5) is then modified to

$$\phi_b = \beta\phi_b^n\left[1 + K_H\frac{\Delta H_i}{H_{fg}}\right] \qquad (9)$$

The slope K in Eqns. (5) and (9) could be determined by choosing an arbitrary value of $(\Delta H_i)_m$ and expressing the corresponding burnout fluxes ϕ_b^m found on the ϕ_b-ΔH_i line in the terms of the parameters in Eqn.(6).

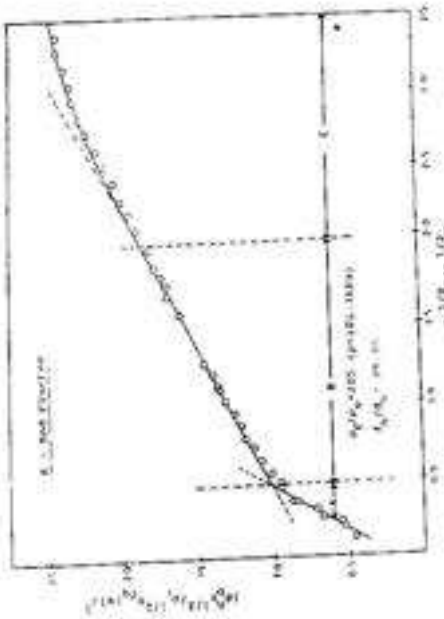

Fig.2: Graphic Representation of 6- rod Cluster ϕ_b^* Data A-, B- and C- Regimes.

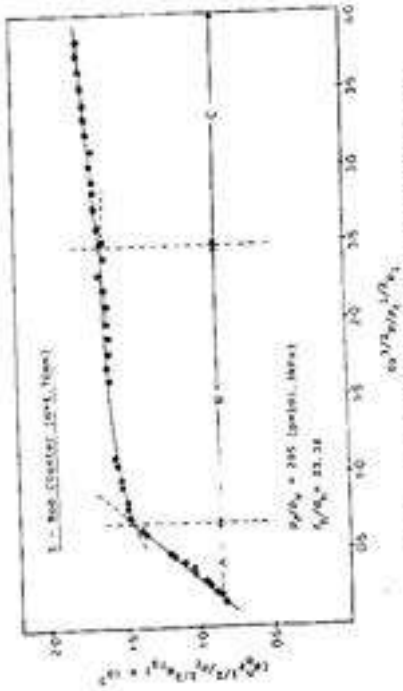

Fig.3: Graphic Representation of 5- Rod Cluster ϕ_b^* Data A-, B- and C- Regimes.

Since ϕ_b^m, is related to ϕ_b^n by Eqn.(5) or (9) as:

$$\phi_b^m = \phi_b^n \left(1 + K_p \frac{(\Delta H_1)_m}{H_{fg}}\right) \quad (10)$$

the slope K_p becomes

$$K_p = \frac{H_{fg}}{(\Delta H_1)_m}\left(\frac{\phi_b^m}{\phi_b^n} - 1\right) \quad (11)$$

ϕ_b^m was correlated in the same way as ϕ_b^n in terms of the dimensionless parameters. Representing the slope at any pressure as K_p with H_{fg} as $(H_{fg})_p$ then Eqn. (11) can be rewritten using the correlated forms:

$$K_p = \frac{(H_{fg})_p}{(\Delta H_1)_m}\left[f_p^m\left(\frac{G_\gamma^{1/2} p}{\rho_l^{1/2} p_1}, \frac{\rho_l}{\rho_v}, \frac{l_h}{d_h}\right)\right] \Big/ \left[f_p^n\left(\frac{G_\gamma^{1/2} p}{\rho_l^{1/2} p_1}, \frac{\rho_l}{\rho_v}, \frac{l_h}{d_h}\right)\right] - 1 \quad (12)$$

Using the experimental result presented in Eqn.(2), ϕ_b^m and ϕ_b^n can be related to the values at 1 bar, ϕ_{b1}^m and ϕ_{b1}^n respectively as:

$$\phi_b^m = \phi_{b1}^m \left(\frac{p}{p_1}\right)^a \text{ and } \phi_b^n = \phi_{b1}^n \left(\frac{p}{p_1}\right)^a \quad (13)$$

Substituting for ϕ_b^m and ϕ_b^n in Eqn. (10) using the expressions (13) gives the expression

$$\phi_{b1}^n \left(\frac{p}{p_1}\right)^a = \phi_{b1}^n \left(\frac{p}{p_1}\right)^a \left(1 + K_p \frac{(\Delta H_1)_m}{(H_{fg})_p}\right) \quad (14)$$

The above equation is valid for any pressure greater than 1 bar, and for 1 bar conditions, it simplifies to the form

$$\phi_{b1}^m = \phi_{b1}^n \left(1 + K_1 \frac{(\Delta H_1)_m}{(H_{fg})_1}\right) \quad (15)$$

Now dividing Eqn.(14) by Eqn.(15), shows that

$$\frac{K_p / (H_{fg})_p}{K_1 / (H_{fg})_1} = \frac{\left\{\left[\left(\phi_{b1}^m \left(\frac{p}{p_1}\right)^a / \phi_{b1}^n \left(\frac{p}{p_1}\right)^a\right) - 1\right]\right\}}{(\phi_{b1}^m / \phi_{b1}^n) - 1} = 1 \quad (16)$$

for a specified cluster geometry in a flow regime where α value remains the same. Thus, the change of K with pressure is given by

$$K_p = \left(\frac{(H_{fg})_p}{(H_{fg})_1}\right) K_1 \quad (17)$$

Eqn.(12) can be modified using fluid properties of Freon-113 at 1 bar [ρ_l/ρ_v = 205, $(H_{fg})_1$ = 145.9kJ/kg] to determine an expression for K_1; leading to

$$K_1 = \frac{(H_{fg})_1}{(\Delta H_1)_m}\left\{\left[f_1^n\left(\frac{G\gamma^{1/2}}{\rho_l^{1/2}}, \frac{l_h}{d_h}\right)\right] \Big/ \left[f_1^n\left(\frac{G\gamma^{1/2}}{\rho_l^{1/2}}, \frac{l_h}{d_h}\right)\right] - 1\right\} \quad (18)$$

Now, it is possible to determine K_p (the slope of ϕ_b - ΔH_1 line for any pressure greater than 1 bar) by relating it to K_1 calculated from Eqn.(18) using expression (17).

In the limited pressure range of the present experiments (101.3 - 165kPa) the variation of H_{fg} is small and therefore, κ in Eqn.(4) is strongly dependent on pressure. Normalling κ and ϕ_b^n yields a coefficient K which is virtually independent of pressure, at least in the tested range.

(i) **Expression for ϕ_b^n**

Two forms of expressions were derived for predicting the values. One form is applicable to data in those flow regimes where $\phi_b^n \gamma^n / \rho_l^n H_{fg}$ vrs. $G\gamma^n p / \rho_l^n p_1$ followed a linear relationship for fixed ρ_l/ρ_v and γ_b/d_b. The other form of equation is valid for regimes where the variation with $G\gamma^n \rho_l^n p_1$ was exponential. It was found out that the variation with ρ_l/ρ_v was exponential and it was stated earlier that the variation with l_b/d_b was assumed to be hyperbolic. Thus the explicit form of Eqn.(6) is either

$$\frac{\phi_b^n \gamma^{1/2}}{H_{fg} \rho_l^{1/2}} = c_1 \left[1 + c_2 \left[\frac{G \gamma^{1/2} p}{\rho_l^{1/2} p_1}\right]\right] \left[1 + c_3 \frac{l_h}{d_h}\right]^{-1} \left[\frac{\rho_l}{\rho_v}\right]^c \quad (19)$$

or

$$\frac{\phi_b^n \gamma^{1/2}}{H_{fg} \rho_l^{1/2}} = k_1 \left[\frac{G \gamma^{1/2} p}{\rho_l^{1/2} p_1}\right]^r \left[1 + k_2 \frac{l_h}{d_h}\right]^{-2} \left[\frac{\rho_l}{\rho_v}\right]^m \quad (20)$$

Eqn.(19) applies to data in flow regimes A and B of even clusters to A and C of the odd-clusters. In flow regime C of even-geometry and B of odd configuration Eqn.(20) is applicable.

Different numerical values of the exponents and coefficients have been obtained for the even- and odd- numbered clusters in each of the three flow regimes. A list of them is provided in Table 2.

In order to determine the parameter β associated with Eqn.(9) when burnout values are within H-(high enthalpy) regime for the C-regime of even-numbered clusters, another burnout value called ϕ_b^* was obtained at the intersect of the H-regime line

Table 2(a) Constants and Exponents of Eqn. (19)

Geometry	Flow Regime	$c_1 \times 10^4$	c_2	$c_3 \times 10^3$	
Even	A	8.96	7.416	1.50	-0.263
	B	17.40	0.857	14.40	-0.112
Odd	A	32.75	2.129	57.60	-0.161
	C	382.50	0.073	7.60	-0.593

Table 2(b) Constants and Exponents of Eqn.(20)

Geometry	Flow Regime	$k_1 \times 10^3$	$k_2 \times 10^3$	ν	
Even	C	2.961	3.60	0.402	-0.110
Odd	B	36.350	7.80	0.080	-0.566

(ii) Expressions for K

Expressions for determining the parameter K (a measure of steepness of the ϕ_b -ΔH_i line were derived to correspond to ϕ_b^* correlated equations (19) and (20). In the light of the preceding discussion, only expressions for the 1 bar condition, K_1 are provided and values at higher pressures in the tested range can be determined using Eqn.(17). If K_1 is simply denoted as K, the expression relevant to the regimes covered by Eqn.(19) is

$$K = c_4\left\{\left[\frac{c_1 + c_2\left(G_\gamma^{1/2}/\rho_\ell^{1/2}\right)}{1 + c_3\left(G_\gamma^{1/2}/\rho_\ell^{1/2}\right)}\right]\left[\frac{1 + c_5(l_h/d_h)^2}{1 + c_7(l_h/d_h)}\right] - 1\right\} \qquad (21)$$

Similarly, for the regimes covered by Eqn.(20)

$$K = k_3\left\{\left(G_\gamma^{1/2}/\rho_l^{1/2}\right)^{\Omega}\left(\frac{\kappa_4 + k_5(l_h/d_h)}{1 + k_6(l_h/d_h)}\right) - 1\right\} \qquad (22)$$

For the C-regime of even-clusters the exponent Ω and constants k_4 - k_6 have different values for the L-(low) and H-(high) enthalpy regimes. The constants associated with Eqns. (21) and (22) are listed in Tables 3(a) and 3(b) respectively.

with the ϕ_b-axis (at $\Delta H_i = 0$, see Fig.4.). Following the same procedure as before ϕ_b^* was correlated in terms of the parameters in Eqn.(6). Since ϕ_b^* is an arbitrary quantity which has no physical significant it was then expressed in terms of ϕ_b° the extrapolated value for L-regime at $\Delta H_i = 0$ and the coefficient β defined as

$$\beta = \phi_b^\circ/\phi_b^n \qquad (23)$$

Thus, from the variations of ϕ_b^* and ϕ_b° in terms of the dimensionless numbers the parameter β simplifies to the form

$$\beta = 1.075\left(\frac{G_\gamma^{1/2}P_1}{\rho_l^{1/2}P_1}\right)^{0.044}\left(\frac{1+0.0036(l_h/d_h)}{1+0.0156(l_h/d_h)}\right) \qquad (24)$$

(iii) Burnout - Exit Quantity (ϕ_b - χ_{ex}) Relationship

In the literature one finds burnout fluxes expressed in terms of exit quantity, χ_{ex}. If we define

$Q_b = \phi_b P_h l_h$, $m = GA_f$ and $d_h = 4A_f/P_h$

then ΔH_i can be replaced by χ_{ex} in Eqn. (1):

$$\frac{\Delta H_i}{H_{fg}} = \frac{4\phi_b}{GH_{fg}d_h}\frac{l_h}{d_h} - \chi_{ex} \qquad (25)$$

Table 3(a) Constants of Eqn.(21)

Geometry	Flow Regime	c_1	c_2	c_4	$c_5 \times 10^3$
Even	A	8.17	2.266	8.630	6.0
	B		1.462	1.207	13.6
Odd	A	8.17	0.992	2.270	36.0
	B		1.198	0.104	4.0

Table 3(b) Constants and Exponents of Eqn.(22)

Geometry	Flow Regime	Enthalpy	k_1	k_2	$k_3 \times 10^1$	$k_4 \times 10^1$	Ω
Even	C	L	9.732	0.965	3.45	-1.0	-0.046
Odd	B	H	8.17	0.906	14.10	-1.0	-0.112
		"		1.204		7.0	0.007

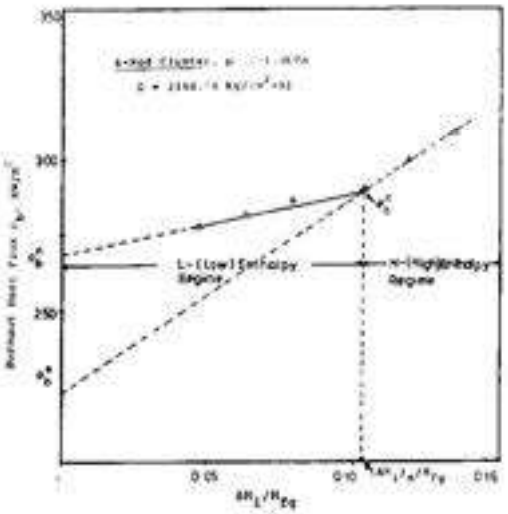

Fig.4: Positions of Burnout Heat Fluxes (ϕ_b^*, ϕ_s^*, ϕ_t^*) of 6-Rod Cluster, C-Regimes.

Multiplying the first term on the RHS by $[\{\gamma^n p\}/\{\rho_l^n p_1\}]/[\{\gamma^n p\}/\{\rho_l^n p_2\}]$ yields

$$\frac{\Delta H_f}{H_{fg}} = \frac{\phi_b \gamma^{1/2}}{H_{fg}\rho_f^{1/2}} \frac{p/p_1}{(G\gamma^{1/2}p/\rho_f^{1/2}p_1)} \frac{l_h}{d_h} - \chi_{ex} \quad (26)$$

Now the term $\Delta H_f/H_{fg}$ in Eqns.(5) and (9) can be eliminated using expression (26). ϕ_b is then made subject of the equations both sides of the equations multiplied by $\gamma^n/H_{fg}\rho_l^n$. The equation corresponding to the linear ϕ_b - ΔH_f relationship of Eqn. (5) becomes

$$\frac{\phi_b \gamma^{1/2}}{H_{fg}\rho_f^{1/2}} = \frac{\chi_{ex} - 1}{\left(+\frac{l_h}{d_h} \frac{p}{p_1} \frac{\chi_L}{G\gamma^{1/2}p/\rho_f^{1/2}p_1}\right) - \left[1/\left(\beta \frac{\phi_b \gamma^{1/2}}{H_{fg}\rho_f^{1/2}}\right)\right]} \quad (27)$$

The identical relation corresponding to Eqn.(9) is given by

$$\frac{\phi_b \gamma^{1/2}}{H_{fg}\rho_f^{1/2}} = \frac{\chi_{ex} - 1}{\left(+\frac{l_h}{d_h} \frac{p}{p_1} \frac{\chi_H}{(G\gamma^{1/2}p/\rho_f^{1/2}p_2)}\right) - \left[1/\left(\beta \frac{\phi_b \gamma^{1/2}}{H_{fg}\rho_f^{1/2}}\right)\right]} \quad (28)$$

It is possible to relate the ϕ_b - χ_{ex} equations in terms of the parameters $G\gamma^n p/\rho_l^n p_1$, ρ_f/ρ_v and l_h/d_h only by substituting the relevant ϕ_b^* expressions for different flow regimes in Eqns.(27) and (28). The relationship corresponding to Eqn.(19) then becomes:

$$\frac{\phi_b \gamma^{1/2}}{h_{fg}\rho_f^{1/2}} = c_1\left[1 + c_2\frac{G\gamma^{1/2}\beta}{\rho_f^{1/2}p_1}\right] \times$$

$$\left[\frac{Kz_{ex} - 1}{4c_1\left[c_2 + 1/\frac{G\gamma^{1/2}\beta}{\rho_f^{1/2}p_1}\right]\left[\frac{\beta}{p_1}\frac{l_h}{d_h}K_H - \left[\frac{c_2 l_h}{d_h} + 1\right]\right]\left[\frac{\rho_f}{\rho_v}\right]^{-\sigma}}\right]$$

(29)

Similarly, the relationship for the flow regimes satisfying Eqn.(20) is

$$\frac{\phi_b \gamma^{1/2}}{h_{fg}\rho_f^{1/2}} = K_1\left[\frac{G\gamma^{1/2}\beta}{\rho_f^{1/2}p_1}\right]^{\nu}$$

$$\left[\frac{Kz_{ex} - 1}{4K_1\left[\frac{G\gamma^{1/2}\beta}{\rho_f^{1/2}p_1}\right]^{\nu-1}\frac{\beta}{p_1}\frac{l_h}{d_h}K_H - \left[k_2\frac{l_h}{d_h} + 1\right]\left[\frac{\rho_f}{\rho_v}\right]^{-\sigma}}\right]$$

(30)

In the H-(high) enthalpy regime of C-flow regime of even numbered rod clusters, substitution of Eqn.(20) in Eqn.(28) followed by rearrangement gives the equation:

$$\frac{\phi_b \gamma^{1/2}}{h_{fg}\rho_f^{1/2}} = 4\beta K_1\left[\frac{G\gamma^{1/2}\beta}{\rho_f^{1/2}p_1}\right]^{\nu}$$

$$\left[\frac{K_H\chi_{ex} - 1}{4\beta K_1\left[\frac{G\gamma^{1/2}\beta}{\rho_f^{1/2}p_1}\right]^{\nu-1}\frac{\beta}{p_1}\frac{l_h}{d_h}K_H - \left[k_2\frac{l_h}{d_h} + 1\right]\left[\frac{\rho_f}{\rho_v}\right]^{-\sigma}}\right]$$

(31)

The ranges of χ_{ex} for the different flow regimes are found from Eqn.(25) using the corresponding values of $\Delta H_i/H_{fg}$. Eqn.(31) should only be used for exit qualities below the point of break in the ϕ_b - χ_{ex} line.

(iv) Criterion for a break in ϕ_b - χ_{ex} relationship

It has been mentioned that for even-numbered peripheral rods in the C-regime (high mass velocity) the relationship between ϕ_b and $\Delta H_i/H_{fg}$ or χ_{ex} is represented by two straight lines with different slopes K_L (low enthalpy and K_H (high enthalpy). The quantity χ_{ex} where these two lines intersect can be found from Eqns. (27) and (28). We denote the slope K_L and the burnout flux $\phi_{b,L}$ in Eqn. (27) and corresponding K_H and $\phi_{b,H}$ in Eqn.(28). For the intersect $\phi_{b,L} = \phi_{b,H}$ yielding:

$$\chi_{ex}^{bt} = \frac{\xi\,(K_H - K_L) + \beta - 1}{\beta K_H - K_L} \qquad (32)$$

where

$$\xi = 4\beta\left(\frac{\phi_b^n \gamma^{1/2}}{h_{fg}\rho_f^{1/2}}\right)\left(\frac{p}{p_1}\right)\left(\frac{l_h}{d_h}\right) \Big/ \left(\frac{G\gamma^{1/2}\beta}{\rho_f^{1/2}p_1}\right)$$

Substituting for $\phi_b{}^n\gamma^n/\rho_f{}^n H_{fg}$ in the expression of Eqn. (20) which satisfies $\phi_b{}^n$ data in the C-regime of even-numbered clusters yields the relationship:

$$\chi_{ex}^{bt} = \frac{4\beta K_1\left[\left[\frac{G\gamma^{1/2}\beta}{\rho_f^{1/2}p_1}\right]^{\nu-1}\left[\frac{\rho_f}{\rho_v}\right]^{\sigma}\left[\frac{l_h/d_h}{1 + k_2(l_h/d_h)}\right]\left[\frac{\beta}{p_1}\right]\right]}{\beta K_H - K_L}$$

$$\frac{\left[K_H - K_L\right] + \beta - 1}{\beta K_H - K_L} \qquad (33)$$

Exit quality values greater than χ_{ex}^{bt} computed from Eqn.(33) would be expected to lie in the L-region whereas smaller ones are associated with H-regime (high subcooling on inlet and hence low quality at exit)

(v) Boundaries for Flow Regions

For the correct selection of the set of equations predicting burnout in a given flow regime the boundaries of this regime must be specified. It is likely that transition regimes exist which lie between the three principal regions presented in the studies of Katto [4] and Dukler [5] and in this work. However, if these transition regimes are neglected then the boundaries between adjacent flow regimes can be obtained by equating the $\phi_b{}^n\gamma^n/\rho_f{}^n H_{fg}$ expressions (19) and (20) relevant to flow regimes A and B and regimes B and C respectively. By following this method we obtain for

(a) Even-numbered Rod Clusters

The boundary between regimes A and B is determined by solving the equation

$$l_h/d_h = (\Gamma - 1)/\left[(c_3)_B - \Gamma(c_3)_A\right] \qquad (34)$$

where

$$\Gamma = \frac{(c_1)_B}{(c_1)_A}\left(\frac{1 + (c_2)_B(G\gamma^{1/2}\beta/\rho_f^{1/2}p_1)}{1 + (c_2)_A(G\gamma^{1/2}\beta/\rho_f^{1/2}p_1)}\right)\left(\frac{\rho_f}{\rho_v}\right)^{t_B - t_A} \qquad (35)$$

The boundary between regimes B and C is determined from

$$l_h/d_h = (\Psi - 1)/\left[(k_2)_C - \Psi(k_2)_B\right] \qquad (36)$$

where

$$\Psi = \frac{(k_1)C}{(c_1)_B}\left(\frac{\left(\frac{G\gamma^{1/2}p}{\rho_l^{1/2}p_1}\right)^{n_C}}{\left(1+(c_2)_B\frac{G\gamma^{1/2}p}{\rho_l^{1/2}p_1}\right)}\right)\left(\frac{\rho_l}{\rho_v}\right)^{n_C-n_B} \quad (37)$$

(b) Odd-numbered Rod Clusters

The boundary between regimes A and B is obtained from

$$l_B/d_h = (\upsilon - 1)/[(k_2)_B - \upsilon(c_2)_A] \quad (38)$$

where

$$\upsilon = \frac{(k_1)B}{(c_1)_A}\left(\frac{\left(\frac{G\gamma^{1/2}p}{\rho_l^{1/2}p_1}\right)^{n_B}}{\left(1+(c_2)_A\frac{G\gamma^{1/2}p}{\rho_l^{1/2}p_1}\right)}\right)\left(\frac{\rho_l}{\rho_v}\right)^{n_B-n_A} \quad (39)$$

Finally for the boundary between B and C flow regimes, the equation that is valid is of the form

$$l_B/d_h = (\Xi - 1)/[(c_2)_C - \Xi(k_2)_B] \quad (40)$$

where

$$\Xi = \frac{(k_1)C}{(c_1)_B}\left(\frac{1+(c_1)_C\left(\frac{G\gamma^{1/2}p}{\rho_l^{1/2}p_1}\right)}{\left(\frac{G\gamma^{1/2}p}{\rho_l^{1/2}p_1}\right)^{n_B}}\right)\left(\frac{\rho_l}{\rho_v}\right)^{n_C-n_B} \quad (41)$$

The subscripts A, B and C in all expressions stand for the flow regimes.

The solution of Eqns. (34 - 41) for $G\gamma^{n}p/\rho_l^{n}p_1$ for Freon-113 at 1 bar are shown in Fig.5 for even-geometry and in Fig.6 for the odd configuration as vertical lines.

DISCUSSION AND CONCLUSION

The equations have been checked against experimental results obtained using the even- and odd-numbered rod clusters in the different flow regimes in Freon-113. On the whole, satisfactory agreement is found between predicted and experimental results. For the clusters of even geometry; the maximum RMS deviation of the experimental values for the A-regime is ±3.8% and the standard deviation ±.77%. Considering the clusters of odd arrangement, the agreement is even better with a maximum RMS of 2.38% and standard deviation of ±2.13%. It can be seen that the deviations for each geometry (even or odd) are quite small and this implies that burnout heat flux are well predicted by a particular set of equations for a certain geometrical pattern of rod-cluster.

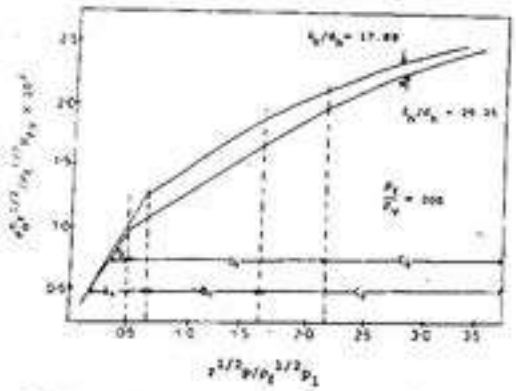

Fig.5: Variation of $\phi_h{}^n\gamma^{1/2}/\rho_l^{1/2}H_{fg}$ with $G\gamma^{1/2}p/\rho_l^{1/2}p_1$ in Flow Regimes of 6-Rod and 4-Rod Clusters (Evens).

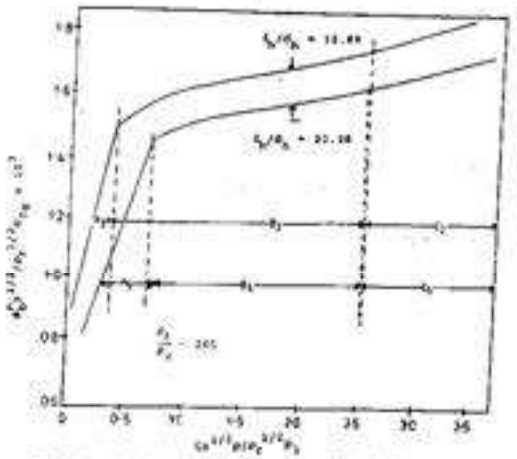

Fig.6: Variation of $\phi_h{}^n\gamma^{1/2}/\rho_l^{1/2}H_{fg}$ with $G\gamma^{1/2}p/\rho_l^{1/2}p_1$ in Flow Regimes of 5-Rod and 3-Rod Clusters (Odd).

No equations were found in the literature which could correspond to the geometrical characteristics of the tested rod clusters at the low pressures used in this study. However, for the characteristics of the present 5-rod and 6-rod clusters, Macbeth [13] derived equation for boiling water at 69 bars (ρ_l/ρ_v = 20.6) and Tong's correlation W-3 [14] for water at 138 bars (ρ_l/ρ_v = 7.2) ought to be suitable for B- and C- flow regimes, albeit at high pressures. In

order to achieve a meaningful comparison, the scaling factors based on Eqn.(5) were used to compute the burnout fluxes at high pressures and then scaled from high pressure to low pressure. The plot of ϕ_b vs. p for water system shown in Collier's [6] book was used to extrapolate the curve for 69 bars and 138 bars to 8.44 bars (corresponding to 1 bar of Freon-113) to obtain the pressure scaling factors of 1.57 and 3.40 respectively.

The burnout heat fluxes obtained in this manner were compared for the even-numbered clusters in Fig.7 and in Fig.8 for odd-numbered cluster with predictions using the equations. The comparison shows reasonable agreement with the correlations in the B-regime and in the low exit quality region of the C-regime as far as the absolute values of ϕ_b are concerned. However, at high flow rates and higher exit qualities, the present results are substantially higher than those predicted by both correlations. This is obviously due to the break and change in slope which is not reflected in the water-correlations developed for high pressure systems. On the other hand, the comparison in Fig.8 shows the anomalous behaviour of the odd-numbered clusters. Since rod clusters in nuclear reactors are normally of the even type therefore will have provided the data on which Macbeth's correlation is based, one would not expect it to predict burnout values for the anomalous clusters correctly.

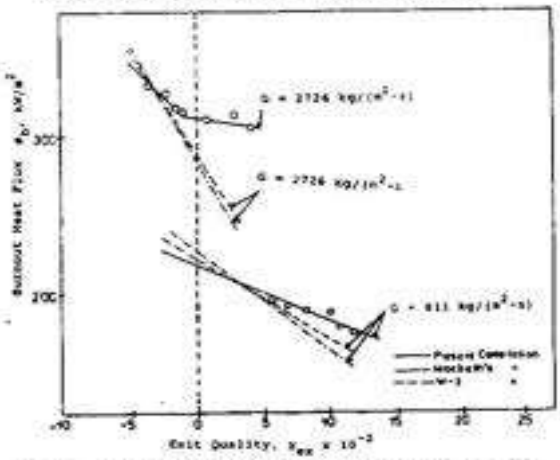

Fig.7: Comparison of Present Correlation with Macbeth's [13] and W-3 [14] for 6-Rod Cluster (Even).

Comparing the equations with Bernath's correlation [1] derived for annuli and Bowring's [15] equation for uniformly heated tubes indicate large deviations in mass velocity regime, as shown in Fig.9. Quali-

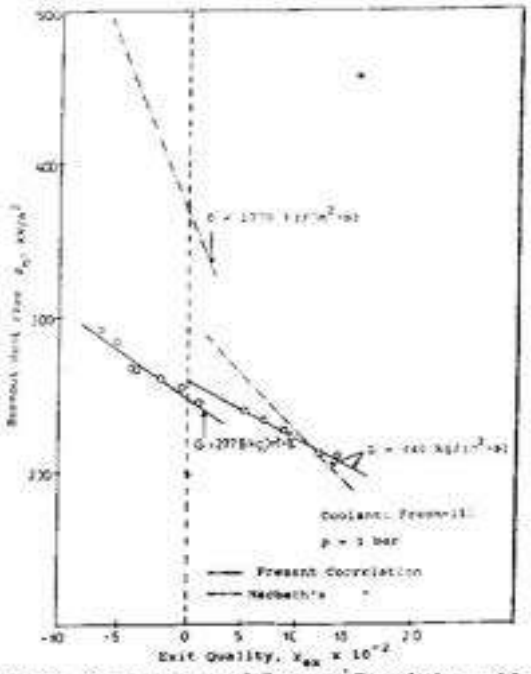

Fig.8: Comparison of Present Correlation with Macbeth's [13] for 5-Rod Cluster (Odd).

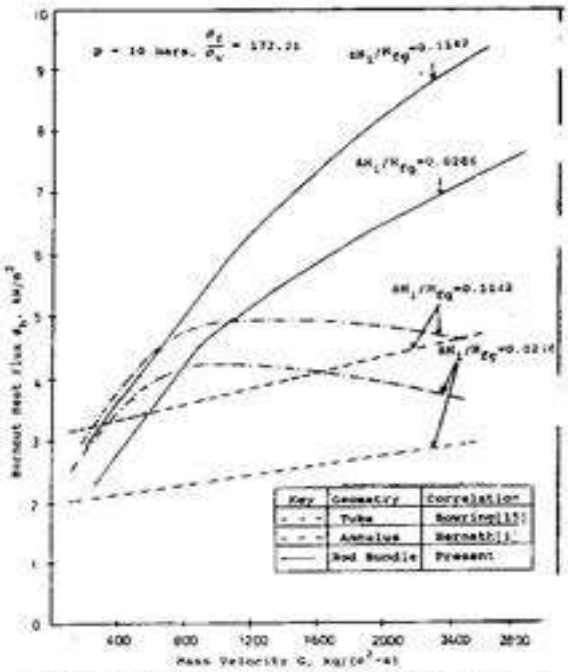

Fig.9: Comparison of Predicted Water Burnout Results Using Present Equation with Correlations for Simpler Geometries (Tubes and Annuli).

tatively, this observation is consistent with the result that burnout data in circular tubes, annuli and rod bundles do not follow the same trend. However, the trends followed by low pressure burnout data in the above mentioned geometries could be confirmed by experiments under low pressure conditions.

The correlating equations were developed in terms of the dimensionless properties suggested in Eqn.(6) for a modelling fluid, Freon-113. In order to assess their more general validity the present correlation must be adopted for other coolants. The original expression $G\gamma^n/\rho_l^n$ proposed by Barnett was modified to $G\gamma^n$ $p/\rho_l^n p_s$. It is hoped that the equations can be used to predict the burnout data for any other saturated fluid in the density ratio, ρ_l/ρ_v = 205 - 125 investigated in this study. Hence, a reference pressure P_{cor} is chosen at which the density ratio is the same as for Freon-113 at 1 bar. i.e ρ_l/ρ_v = 205. This means that the Eqns.(19) and (20) would be substituted by the fluid properties of the coolant.

In order to obtain this more general form the pressure corresponding to ρ_l/ρ_v of 205 is denoted as P_{cor} so that the term $G\gamma^n p/\rho_l^n p_s$ becomes $G\gamma^n p/\rho_l^n p_{cor}$. Now, we could expect that if in different liquids the terms l_h/d_h, ρ_l/ρ_v and $G\gamma^n p/\rho_l^n p_{cor}$ are equal then the term $\phi_b\gamma^n/\rho_l^n H_{fg}$ will be equal too. The parameter K can be determined for any pressure (within the ρ_l/ρ_v range of 205 - 125 in this study) using Eqn.(17) with K_1 becoming K_{cor} and $(H_{fg})_1$ as $(H_{fg})_{cor}$. K_{cor} must be evaluated using fluid properties at p_{cor} (ρ/ρ_v = 205) and $\gamma = d(\rho_l/\rho_v)/dp_{cor}$.

The fluid properties of H_2O, Freon-22 and NH_3 were used for predicting $\phi_b\gamma^n/\rho_l^n H_{fg}$ values from the derived set of equations for ρ_l/ρ_v = 205 and plotted in Fig.10 and for ρ_l/ρ_v = 133 in Fig.11. All calculated values fall on one line together with the Freon-113 data, but for a conclusive proof that equations are universally applicable, experimental data for different fluids are necessary.

In summary, modelling of the burnout heat flux has been demonstrated for even- and odd- numbered peripheral rods. The deviations for each geometry (even or odd) are quite small and this implies that burnout heat fluxes are well predicted by a particular set of equations for a certain geometrical pattern of a rod-cluster.

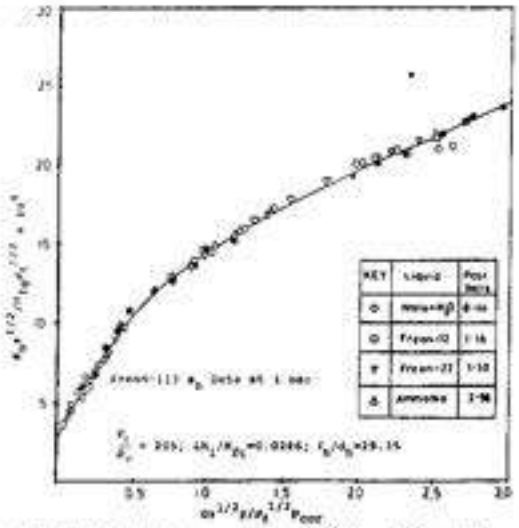

Fig.10: Variation of $\phi_b\gamma^{1/2}/H_{fg}\rho_l^{1/2}$ with $G\rho^{1/2}p/\rho_l^{1/2}p_{cor}$ for ρ_l/ρ_v = 205.

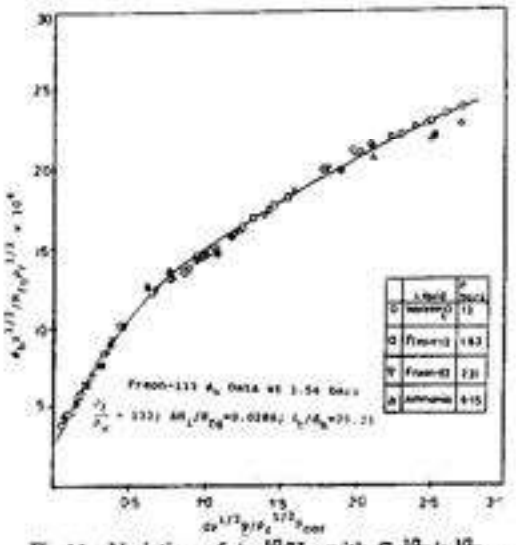

Fig.11: Variation of $\phi_b\gamma^{1/2}/H_{fg}$ with $G\gamma^{1/2}p/\rho_l^{1/2}p_{cor}$ for ρ_l/ρ_v = 133.

5 NOTATION

A_f flow area (m^2)

c_1-c_2 constants in Eqns. (19) & (21)

c_{pl} specific heat at constant pressure, (kJ/kg°C)

d_h heated hydraulic diameter = 4 x flow area/heated perimeter(m).

G mass velocity (kg/m^2-s)

H_{fg} enthalpy of vaporization, (kJ/kg)

ΔH_i enthalpy of subcooling (kJ/kg)

k_l thermal conductivity of liquid (kW/m°C)

k_1 - k_7 Constants in Eqns.(17) and (19)

l_h heated length (m)

$\dot{m}$ mass flow rate (kg/s)

P_h heated perimeter (m)

p absolute pressure (N/m^2)

Q_b burnout power (KW/m^2)

Greek Symbols

β parameter, Eqn.(24)

γ $d(\rho_l\rho_v)/dp_{sat}$ (m^2/N)

ρ_l density of liquid phase (kg/m^3)

ρ_v density of vapour phase (kg/m^3)

ε exponent, Eqn.(19)

σ exponent, Eqn.(20)

ν exponent, Eqn.(20)

ϕ_b burnout heat flux (kW/m^2)

Note:

$$error = \frac{\phi_b\ measured - \phi_b\ predicted}{\phi_b\ measured}$$

$$RMS\ error = \frac{\sqrt{\Sigma(error)^2}}{N}$$

6. REFERENCES

1. Bernath, L., A Theory of Local-Boiling Burnout and Its Application to Existing Data, *Chemical Engineering Progress Symposium* series 56, No.30, pp.95 - 116 (1960).
2. Berger, F.P. and Akaho, E.H.K., Effect of Rod Bundle Geometry (Even-Odd) on Burnout, *Proceedings of 7th International Heat Transfer Conference*, paper FB16, Munich, Ger., pp.267-272 (1982)
3. Macbeth, R.V. Odds and Evens. A Formula for Enhancing the Dryout in Boiling Water Reactor Fuel Channels, UKAEA Report, *AEEW*-R (1994)
4. Katto, Y., General Features of CHF of forced Convection Boiling in Uniformly Heated Vertical Tubes with Zero Inlet Subcooling., *International Journal Heat & Mass Transfer*, Vol.23, pp. 493-504. (1980).
5. Dukler, A.E., Modelling Two Phase Flow and Heat Transfer, *6th Int. Heat Transfer Conference*, Toronto, Canada, Aug.,(1978).
6. Collier, J.G., Convection and Condensation, *McGraw Hill Publishing Corp.*, (1972)
7. Kirby, G.J., Staniforth, R., and Kinneir, J.H., A Visual Study of Forced Convection Boiling, Pt. II, *AEEW-R*281, (1965).
8. Barnett, P.G., The Scaling of Forced Convection Boiling Heat Transfer, *AEEW-R* 134, (1963)
9. Coeffield, Jr., R. D., Rohner Jr., W. M., and Tong, L. S., A Subcooled DNB Investigation of Freon-113 and its Similarity to Subcooled Water DNB Data, *Nuclear Engineering and Design*, Vol.11, pp.143-153, (1969)
10. Jones, J. K., and Hoffman, H. W., Critical Heat Flux of Boiling Water in a rod bundle as a prelude to Boiling Potassium, Paper No. 70-HT-22, *ASME Fluid and Heat Transfer Meeting*, Detroit, (1970).
11. Aladyev, I. T., Gorlor, I. G., Dodonov, L. D., and Fedynsky, O. S., Heat Transfer to Boiling Potassium in Uniformly Heated Tubes, *Heat Transfer-Sov. Res* .1(4). pp.14-26, (1969).
12. Barnett, P. G., Investigation into the Validity of Certain Hypothesis implied by various Burnout Correlations, *AEEW R*-214, (1963).
13. Macbeth R. V., The Burnout Phenomenon in Forced Convective Boiling, *Advances in Chemical Engineering*, Vol.7, pp 207 (1968)
14. Tong, L. S., Prediction of Departure from Nucleate Boiling for an Axially Non-Uni-

form Heat Flux Distribution, *J. Nucl. Energy*, Vol. 21, pp 241-248, (1957).
Bowring, R. W., A Simple but Accurate Round Tube Uniform Heat Flux, Dryout Correlation over Pressure Range 0.7 - 17MN/m^2 (100-2500 psia), *AEEW-R* 789, (1972).